

NMR DIFFUSIONAL COUPLING: EFFECTS OF TEMPERATURE AND CLAY DISTRIBUTION

Vivek Anand, George J. Hirasaki, Rice University, USA
Marc Fleury, IFP, France

This paper was prepared for presentation at the International Symposium of the Society of Core Analysts held in Trondheim, Norway 12-16 September, 2006

ABSTRACT

The interpretation of Nuclear Magnetic Resonance (NMR) measurements on fluid-saturated formations assumes that pores of each size relax independently of other pores. However, diffusional coupling between pores of different sizes may lead to false interpretation of measurements and thereby, a wrong estimation of formation properties. The objective of this study is to provide a quantitative framework for the interpretation of the effects of temperature and clay distribution on NMR experiments. In a previous work, we established that the extent of coupling between a micropore and macropore can be quantified with the help of a coupling parameter (α) which is defined as the ratio of characteristic relaxation rate to the rate of diffusive mixing of magnetization between micro and macropore. The effect of temperature on pore coupling is evaluated by proposing a temperature dependent functional relationship of α . This relationship takes into account the temperature dependence of surface relaxivity and fluid diffusivity. The solution of inverse problem of determining α and microporosity fraction for systems with unknown properties is obtainable from experimentally measurable quantities.

Experimental NMR measurements on reservoir carbonate rocks and model grainstone systems consisting of microporous silica gels of various grain sizes are performed at different temperatures. As temperature is increased, the T_2 spectrum for water-saturated systems progressively changes from bimodal to unimodal distribution. This enhanced pore coupling is caused by a combined effect of increase in water diffusivity and decrease in surface-relaxivity with temperature. Extent of coupling at each temperature can be quantified by the values of α . The technique can prove useful in interpreting log data for high temperature reservoirs.

Effect of clay distribution on pore coupling is studied for model shaly sands made with fine silica sand and bentonite or kaolinite clays. The NMR response is measured for two cases in which clay is either present as a separate, discrete layer or homogeneously distributed with the sand. For layered systems, T_2 spectrum shows separate peaks for clay and sand at 100% water saturation and a sharp $T_{2,cutoff}$ could be effectively applied for estimation of irreducible saturation. However, for dispersed systems a unimodal T_2 spectrum is observed and application of 33ms $T_{2,cutoff}$ would underestimate the irreducible saturation in the case of kaolinite and overestimate in the case of bentonite. The inversion technique can still be applied to accurately estimate the irreducible saturation.

INTRODUCTION

NMR well logging provides a useful technique for the estimation of formation properties such as porosity, permeability, irreducible water saturation, oil saturation and viscosity. The conventional interpretation of NMR measurements on fluid-saturated rocks assumes that the relaxation rate of fluid in a pore is directly related to the surface-to-volume ratio of the pore. In addition, each pore is assumed to relax independently of other pores so that the relaxation time distribution represents a signature of the distribution of pore sizes. Ramakrishan et al (1999) showed that such interpretation often fails if the fluid molecules in intra (micro) and intergranular (macro) pores are diffusively coupled with each other. The pore coupling effects can be particularly enhanced at high formation temperatures and a calibration for the estimation of irreducible saturations based on laboratory data at room temperature may not be suitable.

In a previous work (Anand and Hirasaki, 2005), we demonstrated that the extent of coupling in a pore model consisting of a micropore in contact with a macropore can be quantified with the help of a coupling parameter (α). α is defined as the ratio of characteristic relaxation rate of the pore to the rate of diffusional mixing of magnetization between micro and macropore i.e.

$$\alpha = \frac{\text{Characteristic relaxation rate}}{\text{Diffusion rate}} = \frac{\rho\beta L_2^2}{DL_1} \quad (1)$$

where ρ is the micropore surface relaxivity, β is the microporosity fraction, L_2 is the half length of the macropore and L_1 is the half width of the micropore (refer to figure 1 in reference 2). Numerical simulations show that as α decreases, coupling between micro and macropore increases and the T_2 response of the pore changes from bimodal to unimodal distribution. The amplitude of the faster relaxing (micropore) peak, φ , shows an empirical lognormal relationship with α .

$$\frac{\varphi}{\beta} = \frac{1}{2} \left[1 + \operatorname{erf} \left(\frac{\log \alpha - 2.29}{0.89\sqrt{2}} \right) \right] \quad (2)$$

The pore types can, thus, communicate through three coupling regimes: Total coupling ($\varphi = 0$), Intermediate coupling ($0 < \varphi < \beta$) and Decoupled ($\varphi = \beta$) regime. For systems with unknown physical and geometrical properties, the solution of inverse problem of determining α and β can be obtained from intersection of contours of constant φ and $T_{2,\text{macro}}/T_{2,\mu}$ in α and β parameter space (Figure 17 in reference 2). Here $T_{2,\text{macro}}$ and $T_{2,\mu}$ are the modes of the macropore and micropore peaks at 100% water and irreducible saturation respectively. The model was experimentally validated for pore coupling in several grainstones systems and clay lining pores in sandstones.

The purpose of this paper is to extend the earlier work to describe the effect of temperature and clay distribution on pore coupling. In the first section, a temperature dependent functional relationship of α is proposed by incorporating the temperature

variation of surface relaxivity and fluid diffusion-coefficient. NMR measurements are performed at various temperatures with series of model grainstone systems and reservoir carbonate core at irreducible and 100% water saturation. Measurements at irreducible water saturation show that surface relaxivities for both systems decrease with temperature. The results for 100% water saturated systems illustrate that as temperature is increased, T_2 distributions gradually transition from bimodal to unimodal spectra suggesting an increase in pore coupling with temperature. Estimation of α theoretically predicts the transition of the systems between coupling regimes as temperature is increased. In the second section, diffusional coupling between free and irreducible water in shaly sands is studied as a function of distribution of clays with the sand. Model shaly sands are prepared in two ways such that the clays are either homogeneously dispersed with sand or present as a separate, discrete layer. NMR measurements at 100% and irreducible water saturation show that the free and irreducible water can be diffusively coupled or decoupled depending on the spatial separation between them.

EFFECT OF TEMPERATURE ON DIFFUSIONAL COUPLING

Relaxation rates of bulk fluids are strongly temperature sensitive due to the thermal modulation of translational and rotational correlation times. For fluids in porous media, relaxation is usually dominated by surface relaxation which can be temperature dependent. In addition, diffusional coupling between pores of different sizes can also increase with temperature due to increased diffusional transport of fluid molecules. Thus, the interpretation of temperature effect on NMR measurements in porous media needs to take into account the temperature variation of both surface relaxation and diffusional coupling.

The effect of temperature on pore coupling can be quantified by incorporating the temperature dependencies of surface relaxivity and diffusion coefficient in the functional relationship for α . Surface relaxation of fluid molecules in porous media is governed by two processes (Godefroy et al, 2001). First, translational motion of the fluid molecules near the paramagnetic sites at pore surface and second, exchange between surface and bulk molecules. The temperature dependence of surface relaxation arises from the thermal activation of the translational motion at the pore surface as well as increased exchange between surface and bulk fluid molecules. Quantitatively, the temperature dependence can be expressed as an Arrhenius relationship

$$\rho = \rho_0 \exp\left(\frac{\Delta E}{RT}\right) \quad (3)$$

where ΔE is the effective activation energy and R is the universal gas constant. Self-diffusion of bulk fluids is also a thermally activated process and the diffusion coefficient usually shows Arrhenius dependence with temperature,

$$D = D_0 \exp\left(-\frac{E_a}{RT}\right) \quad (4)$$

In the above equation, E_a is the activation energy for the diffusion process and D_0 is the diffusion coefficient at infinite temperature. Substituting equations (3) and (4) in the

expression for α (equation 1) and grouping variables, a temperature dependent functional relationship of α can be given as

$$\alpha = \alpha_o \exp\left(\frac{E_a + \Delta E}{R} \left(\frac{1}{T} - \frac{1}{T_o}\right)\right) \quad (5)$$

where α_o is the value of coupling parameter at reference temperature T_o . Thus, pore coupling can either increase or decrease with temperature if the difference in the activation energy for diffusion and relaxation process ($E_a + \Delta E$) is positive or negative, respectively.

Experimental Validation

The effect of temperature on NMR diffusional coupling is experimentally studied for two systems of porous media. The first system consists of a homologous series of microporous silica gels with varying grain diameters. The second system consists of a reservoir carbonate core with bimodal pore size distribution. For both systems NMR measurements are performed at total and irreducible water saturation as a function of temperature.

Silica Gels

Silica gels with mean grain radii of 118 μ m (Medium Coarse), 55 μ m (Very Fine) and 28 μ m (Silt size) were obtained from Sigma Aldrich. The physical properties of the gels are given in Table 2 of reference 2. Figure 1 shows the T_2 distributions at 100% water saturation for the three silica gels at 30, 50, 75 and 95°C. At each temperature, the distributions are normalized with the pore volume (area under the curve) to account for the Curie Law. Figure 2 shows the normalized T_2 distributions at irreducible condition for the medium coarse silica gel at the above mentioned temperatures. The NMR apparatus has a response around 1 ms at high temperatures which has been subtracted from the distributions.

The increase in relaxation time at irreducible condition with temperature (Figure 2) shows that the surface relaxivity decreases as the temperature is increased. This result is in agreement with those obtained by Ramakrishnan et al (1999) who saw a similar increase in the relaxation time of water-saturated systems with temperature. The temperature behavior at 100% water saturation can now be interpreted keeping in mind the negative dependence of relaxivity on temperature. Each of the three silica gels in Figure 1 represents a different coupling scenario. The medium coarse silica gel is almost in decoupled regime ($\phi/\beta = 0.97$) at 30°C. As the temperature is increased, surface relaxivity decreases and diffusivity of water increases. As a result, coupling between micro and macropores increases and the system transitions from almost decoupled to intermediate coupling regime. This is evidenced by the reduction in the amplitude of the micropore peak and decrease in the relaxation time of the macropore with temperature. Very fine silica gel is in intermediate coupling regime at 30°C ($\phi/\beta = 0.24$). Increasing the temperature increases coupling so that the T_2 distribution changes from bimodal at 30°C to unimodal at higher temperatures. However, the increase in relaxation rate of the

macropore due to coupling is exactly cancelled by the decrease in surface relaxation and thus the position of macropore peak remains unchanged. Silt size silica gel has a unimodal T_2 distribution at 30°C suggesting that the system is in total coupling regime ($\phi/\beta \sim 0$). Increase in temperature has no further effect on coupling but the corresponding decrease in surface relaxivity leads to a shift of T_2 distribution to longer relaxation times. The results demonstrate that temperature can have apparently different effects on the NMR response even though the systems may be governed by similar principles.

Reservoir Carbonate Core

The carbonate core studied is a Thamama reservoir carbonate with porosity 21.2% and water permeability of 13mD. Analysis of lithology shows that the carbonate is a packstone/wackestone with mainly moldic macroporosity in leached areas. The microporosity is predominantly inside pellets and mud. Figure 3 shows the T_2 distributions of the core at 100% and irreducible water saturation (oil saturated) for three temperatures of 25, 50 and 80°C. We can see that for 100% water-saturated core, as the temperature is increased amplitude of the micropore peak and relaxation time of the macropore decrease. This suggests that diffusional coupling between micro and macropores is increasing with temperature. Similar to the case for silica gels, the increase in pore coupling is due to increase in water diffusivity as well as decrease in surface relaxivity with temperature. The latter claim is based on the fact that the relaxation time of the residual water in the micropores of oil saturated core increases with temperature (lower panel of figure 3). An important implication of the results is that application of a sharp $T_{2,cutoff}$ based on a laboratory calibration at room temperature for the estimation of irreducible saturation may not be suitable for high temperature formations.

Discussion

Effect of temperature on pore coupling for the two systems can be analyzed quantitatively from the temperature variation of α . For silica gels, α at different temperatures can be calculated by including the temperature dependence of surface relaxivity and diffusivity in the definition of α for grainstone systems (Anand and Hirasaki, 2005),

$$\alpha_{\text{grain}}(T) = \frac{\rho(T)\beta R_g^2}{D(T)R_\mu} \quad (6)$$

Here R_g is the grain radius and R_μ is the micropore radius (75 Å for silica gels). The temperature variation of surface relaxivity is obtained from measurements at irreducible saturation (Figure 2). The estimates of self-diffusion coefficient of water as a function of temperature are obtained from the experimental data of Holz et al (2000). For the carbonate core, α is calculated using the inversion technique described earlier. Figure 4 shows the cross plot of the normalized micropore-peak amplitude (ϕ/β) with α for the three silica gels and carbonate core. It can be seen that α accurately predicts the transition of the different coupling regimes with temperature as the systems move downward along the empirical relationship (Equation 2). The microporosity fraction, estimated using the inversion technique, agrees within 5% average absolute deviation as shown in Figure 5.

Thus, the technique can prove useful in accurately estimating formation properties for reservoirs at elevated temperatures.

EFFECT OF CLAY DISTRIBUTION ON PORE COUPLING

NMR well logging has evolved as a promising technology for the formation evaluation of shaly sands. Coates et al. (1994) proposed that the fast relaxing components of the T_2 spectrum in clayey rocks can be attributed to the water adsorbed on clays. This idea was further extended by Prammer et al. (1996) who found that clays in sandstones exhibited specific transverse relaxation times proportional to their surface area and cation exchange capacity (CEC). Thus, they postulated that the position of fast relaxing T_2 peak can be used for clay typing. This claim was disputed by Matteson et al. (2000) who found that relaxation time of clay brine slurries is a function of compaction of clays. Since the degree of compaction of formation clays is usually not known, they argued that clay typing from T_2 measurements alone is not possible. In addition, they found that distinct peaks for clay bound and free water were not visible for the clay-brine slurries.

In order to understand the phenomenological factors causing the apparent differences, a systematic study of the relaxation characteristics of clay-sand systems was undertaken. Two systems of model shaly sands consisting of varying amount of either kaolinite or bentonite clay and fine sand were prepared. In the first system, the clays were uniformly dispersed (dispersed systems) with the sand such that the clays occupied the interstitial voids between the sand grains. For the second system, clays were present as a separate, discrete layer with the sand (laminated systems). NMR response of the systems was measured at 100% and irreducible water saturations.

Experimental Section

Fine sand (grain radius 50 μ m), kaolinite and bentonite clays were obtained from Sigma Aldrich. The physical properties of the materials are given in Table 1. The dispersed and laminated systems were prepared in three sets such that the clay (either kaolinite or bentonite) constituted 0, 2, 5 and 10% of the total solid content. For each set, the systems were prepared at total and irreducible water saturation separately. The details for the preparation of the systems are included below.

Dispersed System

To prepare the dispersed system at 100% water saturation, 15 grams of fine sand was taken in a plastic centrifuge tube. The amount of either clay required to make the desired weight percentage content was added to the sand and the mixture was vigorously shaken to disperse the clay in the interstitial voids between the sand grains. 5 ml of 0.1M calcium chloride solution was added to the mixture to make thick slurries. The slurries were mixed with a glass rod to further homogenize the clays with the sand and then compacted at a relative centrifugal force (RCF) of 1500g. The small amount of supernatant water obtained after centrifuging was removed.

The dispersed systems at irreducible conditions were made by first preparing the water saturated slurries in a 1'' by 1'' teflon sleeve. The base of the sleeve was sealed with a covering of teflon tape. 15 grams of sand and desired amount of either clay were mixed in the sleeve and the mixture was saturated with 5 ml of CaCl₂ solution. The slurries were then centrifuged in a Beckman rock core centrifuge at an air/water capillary pressure of 50psi (which also approximately corresponds to 1500g RCF) for 3 hours to drain the free water. The teflon base is permeable to water but prevents any grain loss during centrifugation.

Laminated System

15g of fine sand and 15ml calcium chloride solution were taken in a centrifuge tube and compacted at 1500g RCF for half hour. The required amount of either clay was added to the sand and centrifuged for 3 hours to compact the systems. Since the sand had already settled before the introduction of clay, there was no elutriation of the clay with sand. Clay, thus, compacted as a laminated layer on top of the sand.

Laminated systems at irreducible conditions were prepared analogously to the dispersed systems at irreducible condition. 15 grams of sand was allowed to settle gravimetrically in 15ml calcium chloride solution in a 1'' by 1'' sleeve with a sealed base. The required amount of either clay was added to the sand and the systems were centrifuged at 50psi air/brine capillary pressure to drain the free water.

Results and Discussion

Fig 6 and 7 show the T_2 distributions of the dispersed and laminated kaolinite systems at 100% water saturation. Figures 8 and 9 show the corresponding distributions for the dispersed and laminated bentonite systems. For each case, the distributions at irreducible conditions are also shown for comparison. Analysis of the T_2 distributions in figures 6-9 shows that the systems exhibit different relaxation characteristics when the clays are dispersed or layered with sand. For the dispersed systems, the T_2 distributions at 100% water saturation show unimodal spectra. The laminated systems, on the other hand, show bimodal T_2 distributions at 100% water saturation. The fast and slow relaxing peaks in the bimodal distributions correspond to water in the clay and sand layer respectively. Note that the faster relaxation of water in bentonite (~4 ms) compared to that in kaolinite (~25ms) is due to the large interlayer surface area in swelling bentonite clay. Bimodal T_2 distributions for the laminated systems indicate that water populations in the clay and sand layer are decoupled. On the other hand, unimodal T_2 distributions for the dispersed systems indicate that water in the interstitial pores between clay and sand is diffusionally coupled. Figure 10 shows that the relaxation rate of water in dispersed systems shows a linear dependence with the clay content. Extrapolation of the linear relationship to zero clay fractions has an intercept close to the relaxation rate of water in sand-only system. Thus, the relaxation rate of water in the dispersed systems can be expressed as

$$\frac{1}{T_2} = \frac{\rho_{\text{sand}} S_{\text{sand}} + \rho_{\text{clay}} S_{\text{clay}}}{V_{\text{total}}} \quad (7)$$

where $\rho_{\text{sand}}S_{\text{sand}}$ and $\rho_{\text{clay}}S_{\text{clay}}$ are the products of relaxivity and surface area for sand and clay respectively and V_{total} is the total volume of water. Since the relaxation rate is simultaneously influenced by both clay and sand surface areas, we do not observe distinct peaks for irreducible and free water.

A quantitative estimate of characteristic lengths required for the systems to be in coupled or decoupled regime can be obtained from the analysis of α for the systems. For coupled systems, α is given as (Anand and Hirasaki, 2005)

$$\alpha = \frac{\rho S_{\text{active}}/V_{\text{total}}}{D/L_2^2} \quad (8)$$

Since the surface area of the sand is negligible compared to that of the clays, relaxation at the surface of the sand grains can be neglected in comparison to that on the clay surface

$$\rho S_{\text{active}} \approx \rho_{\text{clay}} S_{\text{clay}} \quad (9)$$

For total coupling regime α is less than 1. Thus,

$$L_2 < \sqrt{\frac{DV_{\text{total}}}{\rho_{\text{clay}} S_{\text{clay}}}} \quad (10)$$

for totally coupled regime. For decoupled regime α is greater than 50 (based on $\phi/\beta = 0.97$ in equation 2). Thus,

$$L_2 > \sqrt{\frac{50DV_{\text{total}}}{\rho_{\text{clay}} S_{\text{clay}}}} \quad (11)$$

for decoupled regime. From the values of relaxivity and surface area of the clays (Table 1), we find that the characteristic diffusion length for total coupling regime should be less than $15\mu\text{m}$ and $5\mu\text{m}$ for kaolinite and bentonite respectively. Since these values are of the order of the interstitial pores between the sand grains with grain radius of $50\mu\text{m}$, irreducible and free water in dispersed systems are coupled with each other. For the decoupled regime, the diffusion length should be greater than $110\mu\text{m}$ and $35\mu\text{m}$ for kaolinite and bentonite respectively. Since the separation between clay and sand layer is of the order of two centimeters in the laminated systems, we observe distinct peaks for the irreducible clay water and free water.

Estimation of Irreducible water saturation

Irreducible water for the sand-clay systems consists of both clay bound and capillary bound water. The two populations are in close physical proximity and thus, relax at same rates due to fast diffusional exchange (Allen et al, 1998). If, however, the distance between the irreducible and free water is large, the two populations can relax independently with distinct relaxation times. This was experimentally demonstrated for the laminated systems which showed separate peaks for clay and sand layers at 100% water saturation. Thus, for laminated systems a sharp cutoff is applicable to partition the T_2 distributions into the irreducible and free water fractions.

Note that in the model shaly sands considered in this study, there will be an overestimation of irreducible water if a sharp $T_{2,\text{cutoff}}$ is applied at the valley between clay and sand peak. This is due to the additional compaction of the clays during centrifugation as the water squeezes out of the clay layer.

The dispersed systems, on the other hand, are in coupled regime and the application of a sharp $T_{2,\text{cutoff}}$ to estimate the irreducible water would give wrong estimates. For example, application of conventional 33 ms cutoff would overestimate the irreducible saturation in the case of bentonite and underestimate in the case of kaolinite particularly for cases with high clay content. The coupled response necessitates the application of inversion technique for accurate estimation of irreducible saturation. Since the systems are in total coupled regime, the irreducible saturation is given by the ratio of modes of relaxation time peaks at irreducible saturation and 100% water saturation (Anand and Hirasaki, 2005),

$$\beta = \left(\frac{T_{2,\mu}}{T_{2,\text{macro}}} \right)_{\alpha < 1} \quad (12)$$

Figure 11 shows the cross plot of the irreducible saturation obtained using equation (12) with that obtained experimentally from NMR measurements at irreducible saturation. The estimates fall within 4% of the average absolute deviation proving the applicability of the technique. The higher irreducible saturation for bentonite systems than for kaolinite is due to the presence of interlayer water.

These experiments also explain the apparent differences in the results reported by Matteson et al (2000) and Prammer et al (1996). The absence of peak at fast relaxation time for the clay slurries which can be interpreted as clay bound water is due to fast diffusional exchange between clay bound and free water. However, when clays are present as laminated layers or as pore filling masses, the separation between irreducible water and free water is large enough to decouple the NMR responses. Thus, some sandstones can display distinct peaks for clay and free water with the clay response being proportional to the CEC of the clay, as was indeed observed by Prammer et al (1996).

CONCLUSIONS

NMR diffusional coupling between micro and macropores is studied for the effects of temperature and clay distribution. The effect of temperature on pore coupling is quantified by incorporating the temperature dependence of surface relaxivity and diffusion coefficient in the definition of coupling parameter (α). NMR measurements with model grainstones and carbonate core show that the systems transition to more strongly coupled regimes with rise in temperature. This increase in coupling is quantified by a decrease in values of α with temperature. The results also explain the anomalous decrease in relaxation time of macropore with temperature even as relaxivity decreases. Inversion technique is applied to obtain accurate estimates of irreducible saturation for the systems at all temperatures.

Diffusional coupling between irreducible and free water in shaly sands is determined by the distribution of clays with the sand. Experiments with model shaly sands show that irreducible and free water are coupled when clays are dispersed with sand and decoupled when clays form a lamination on sand. From the values of α required for systems to be in coupled and decoupled regimes, a quantitative estimate of the characteristic diffusion lengths can be obtained. Application of inversion technique accurately estimates irreducible saturation for the dispersed case.

REFERENCES

- 1) Allen, D.F. et al. (1998), "Petrophysical Significance of the Fast Components of the NMR T_2 spectrum in Shaly Sands and Shales", *SPE 49307*, SPE ATCE, LA
- 2) Anand, V. and Hirasaki, G.J. (2005), "Diffusional Coupling between Micro and Macroporosity for NMR Relaxation in Sandstones and Grainstones", *Proceedings of SPWLA 46th Annual Logging Symposium*, New Orleans, LA.
- 3) Coates, G.R. et al (1994), "Applying Pulse Echo NMR to Shaly Sand Formation Evaluation", *paper presented at 1994 SPWLA Convention*, Tulsa, Oklahoma.
- 4) GodeFroy, S. et al. (2001), "Temperature Effect on NMR Surface Relaxation", *SPE 71700*, presented at SPE ATCE, LA (30 Sep-3 Oct).
- 5) Holz, M. et al (2000), "Temperature dependent self-diffusion coefficients of water and six selected molecular fluids for calibration in accurate ^1H NMR PFG measurements", *Physical Chemistry Chemical Physics*, Web published, 3rd October.
- 6) Matteson, A. et al (2000), "NMR Relaxation of Clay/Brine Mixtures", *SPE Reservoir Eval & Eng*, 3(5), 408-413.
- 7) Prammer, M.G. et al (1996), "Measurements of Clay-Bound Water and Total Porosity by Magnetic Resonance", *The Log Analyst*, 37, No 6, 61.
- 8) Ramakrishnan, T.S. et al (1999), "New Interpretation Methodology Based on Forward Models for Magnetic Resonance in Carbonates", *Proceedings of SPWLA 40th Annual Logging Symposium*, May 30-June 3.

ACKNOWLEDGEMENTS

The authors would like to acknowledge US DOE DF-PS26-04NT1551 and the Consortium on Processes in Porous media (Baker Hughes, BP, Chevron Texaco, Conoco Philips, Core Labs, Exxon Mobil, Halliburton, Kerr McGee, Marathon, Oil Chem, PTS Labs, Schlumberger, Shell and Statoil) for the financial support.

Table 1: Physical Properties of Fine Sand, Kaolinite and Bentonite clays.

	Sand	Kaolinite	Bentonite
Surface Area (m ² /g)	0.2	19	38
Relaxivity (μm/sec)	4.7	1.4	9.2

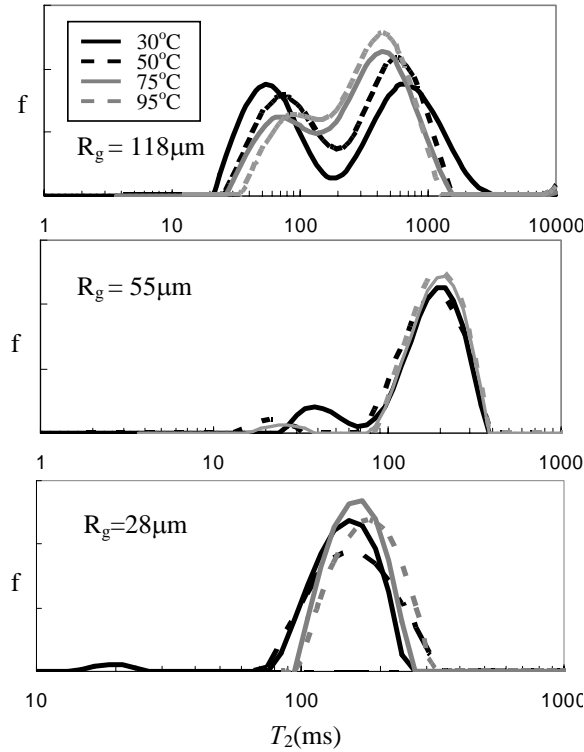


Fig 1: T_2 distributions of silica gels at 100% water saturation and at 30, 50, 75 and 95°C.

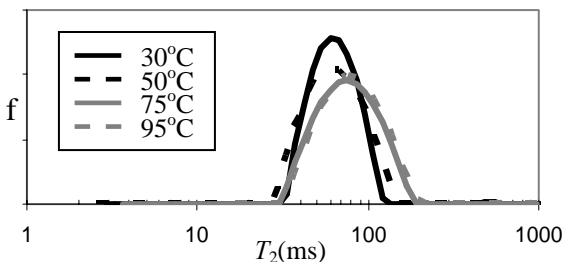


Fig 2: T_2 distributions of the medium coarse silica gel at irreducible water saturation and at 30, 50, 75 and 95°C.

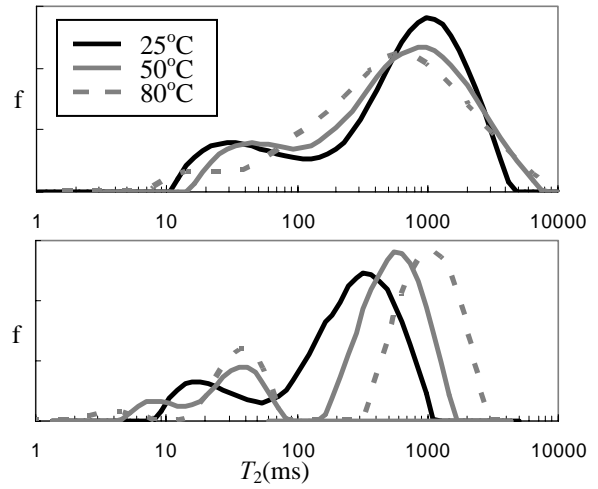


Fig 3: T_2 distributions of the Thamama formation carbonate core at 100% water saturation (upper panel) and irreducible water saturation (lower panel) at 25, 50 and 80°C.

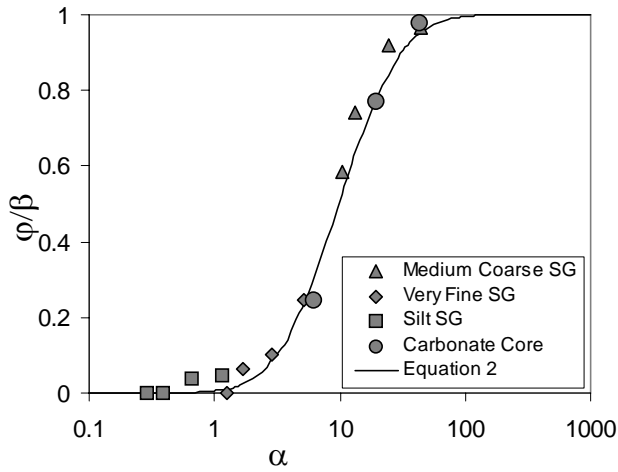


Fig 4: Cross plot of normalized micropore peak amplitude for different systems with α .

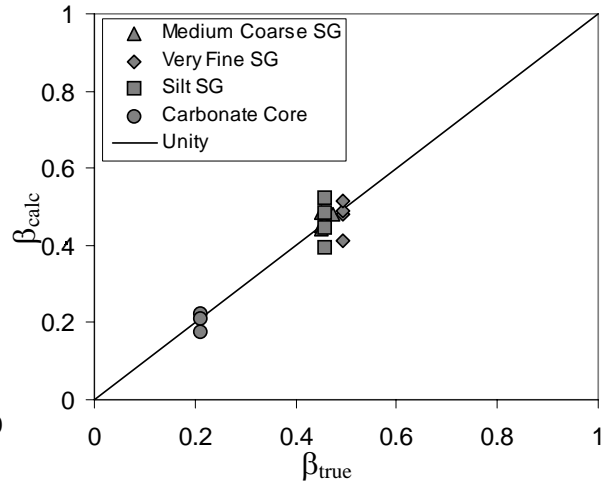


Fig 5: Comparison of the microporosity fraction calculated using the inversion technique and measured experimentally for silica gels and carbonate core.

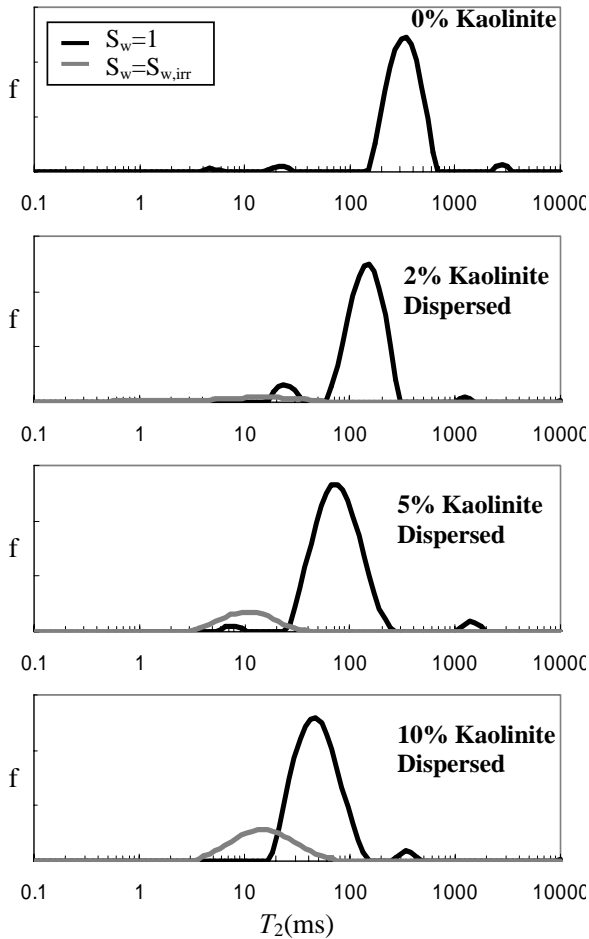


Fig 6: T_2 distribution of dispersed kaolinite-sand systems for different clay weight fractions.

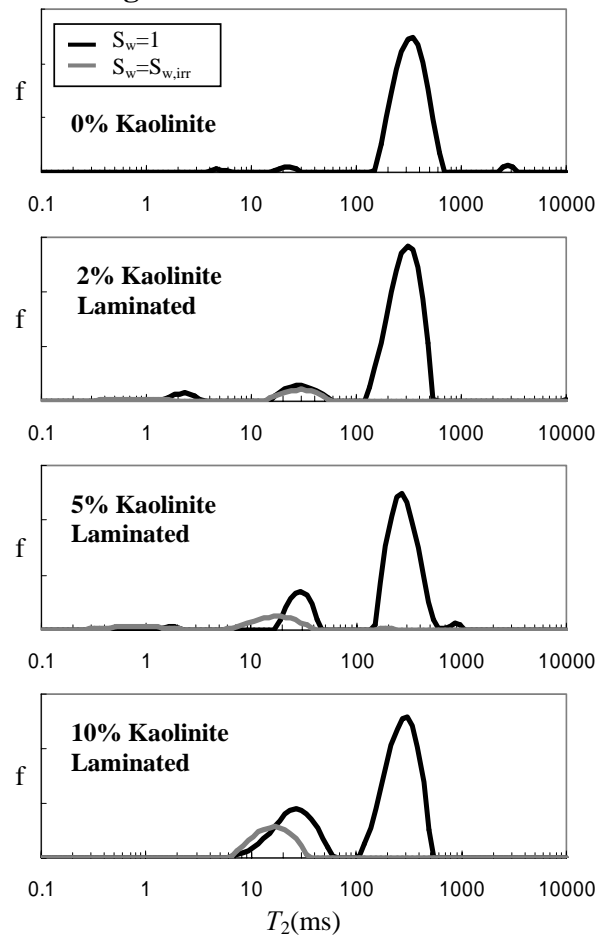


Fig 7: T_2 distributions of laminated kaolinite-sand systems for different clay weight fractions.

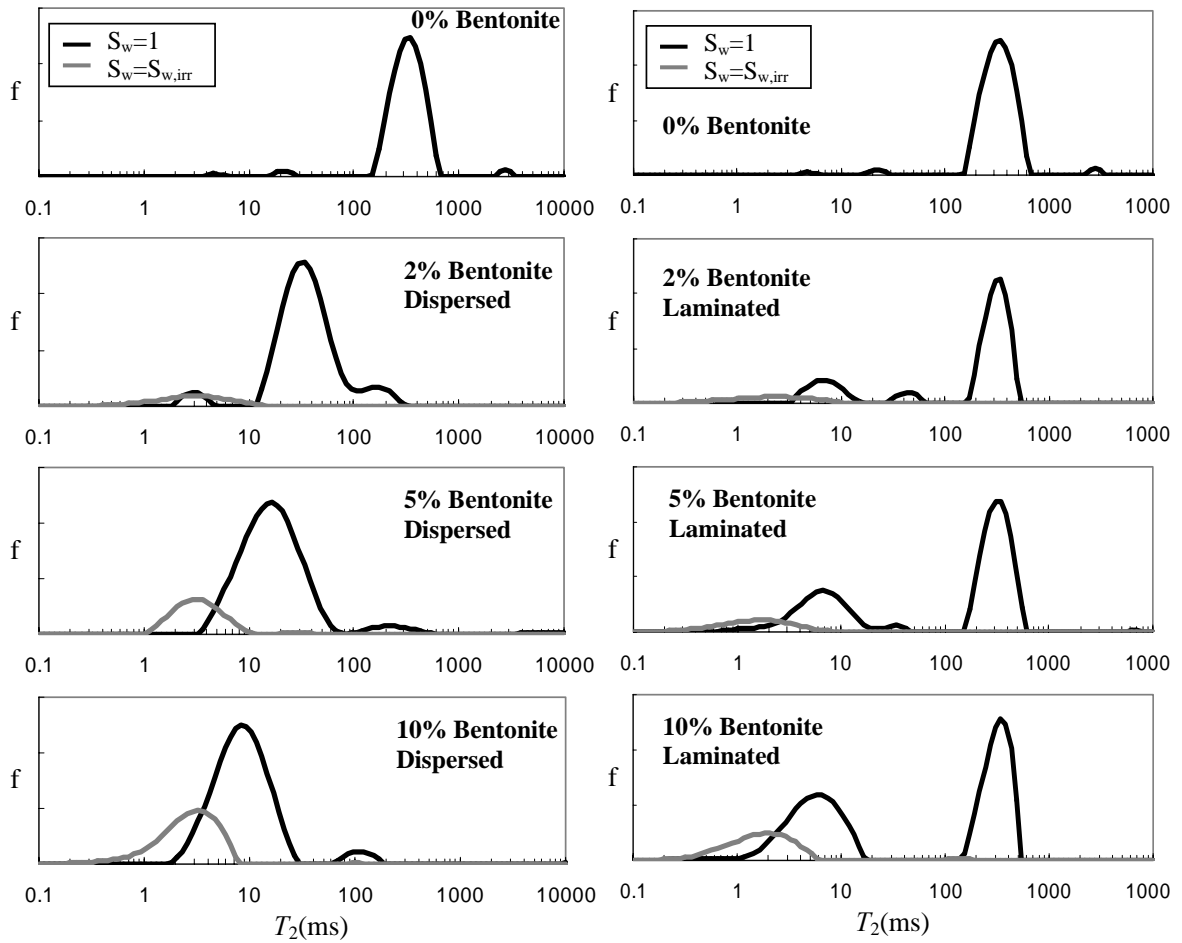


Fig 8: T_2 distributions of dispersed bentonite-sand systems for different clay weight fractions.

Fig 9: T_2 distributions of laminated bentonite-sand systems for different clay weight fractions.

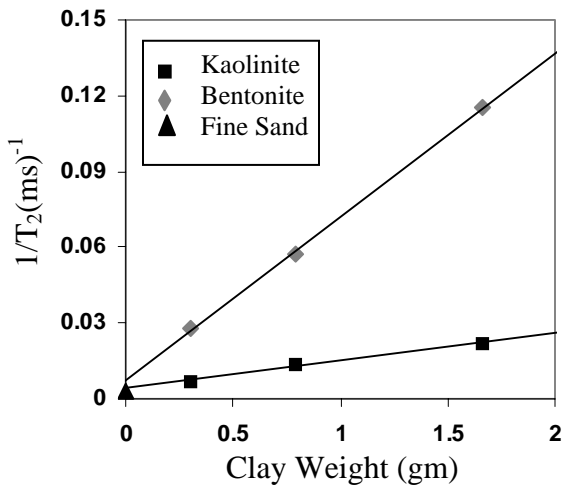


Fig 10: Linear dependence of the relaxation rates of dispersed clay-sand systems with the clay content.

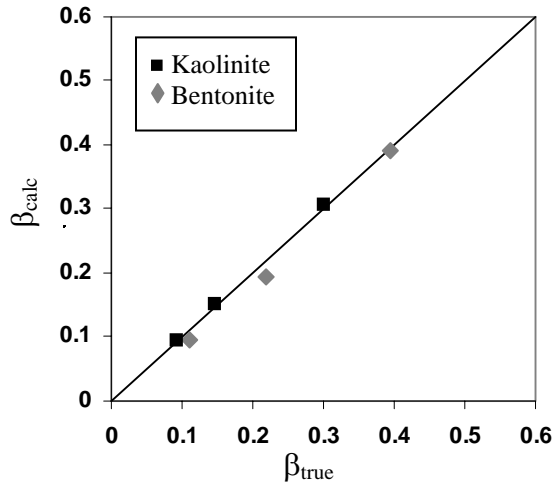


Fig 11: Comparison of the irreducible water saturation calculated using the inversion technique and measured experimentally for dispersed systems.